

# Keplerian Ensemble Approximation. The issue of motions of compact objects in Galactic halo

Łukasz Bratek<sup>1</sup>, Joanna Jałocha<sup>1</sup>, Szymon Sikora<sup>2</sup>, Marek Kutschera<sup>2</sup>

<sup>1</sup>*Institute of Nuclear Physics, Polish Academy of Sciences, Radzikowskiego 152, PL-31342 Kraków, Poland*

<sup>2</sup>*Institute of Physics, Jagellonian University, Reymonta 4, PL-30059 Kraków, Poland*

9 February 2012

## ABSTRACT

The motion of compact objects in Galactic halo is investigated in the approximation of point mass under the assumption that the external halo is not gravitationally dominating and consists of test bodies. Then, the phase space distribution function is that of a spherically symmetric collection of confocal elliptical orbits of various energies and eccentricities, called Keplerian ensemble, and can be determined in a systematic way from the radial velocity dispersion profile of the halo objects. In particular, the anisotropy of the velocity dispersion tensor becomes a function of Galactocentric distance. We find that the observed motion of halo objects can be made consistent with Galaxy mass of  $2.1 \times 10^{11} M_{\odot}$ .

## 1 INTRODUCTION

Galaxy is customarily modeled as a composition of several sub-systems described by simple mass profiles: the central bulge and a spheroid of stars and gas, the galactic disk and an extended external halo. The halo is assumed to consist of nonbaryonic dark matter (NDM) mainly, whereas ordinary matter makes up only a small fraction of the halo. In this picture, NDM dominates the gravitational potential at larger radii.

There are large discrepancies in the estimates of Galaxy mass and uncertainties in its distribution. The available data cannot discriminate between various mass models. Tenths of Galaxy mass estimates are given to chose from, depending on the particular halo model, its free parameters, and the choice of satellites assumed gravitationally bound to Galaxy. A good deal of this indeterminacy lies in the mass-anisotropy degeneracy characteristic of halo models. This uncertainty concerns mainly the non-baryonic dark matter (NDM) halo. There are opinions that the mass distribution is the most poorly known and controversial Galactic characteristic at large distances (Brown et al. 2010) and that the halo issue is entirely speculative (Dehnen & Binney 1998). The problem of NDM concerns various scales of distances. In the Galaxy interior its presence can be inferred from the rotation curve, the vertical gradient of the rotation and from gravitational microlensing (there are also attempts at direct detection of NDM in Earth based experiments), whereas at larger distances, NDM presence is inferred from the motions of compact objects in the external halo.

Except for the habitual argumentation for an extended and massive NDM halo, there is also a premise for not considering it, at least in the Galaxy interior. The high vertical gradient of rotation above the disk midplane can be explained in the thin disk model approximation (Jałocha et al. 2010) (whereas spherical symmetry spoils this agreement). Moreover, in a related finite width disk model, the amount of mass ascertained through microlensing inside the Sun's orbit is found consistent with the dynamical mass inferred from rotation in the same region (Sikora et al. 2011). The two observations suggest that the overall mass distribution might be

flattened rather than spheroidal. Furthermore, the influence of interstellar magnetic fields on rotation of gas can be responsible for flattening of rotation curves at larger radii beyond the visible galactic disks (Battaner et al. 1992), which is ignored in modeling of rotation curves. In this context it is worth to mention that the characteristic rise in the mass-to-light ratio profile (interpreted as a signature of NDM) could be reduced when the magnetic effect was taken into account (Jałocha et al. 2011). What is more, recent independent experiments aimed at the search for dark matter consisting of weakly interacting massive particles, detect no trace of dark matter signal (Ackermann & et al. 2011) and exclude generic WIMP candidates for dark matter (Geringer-Sameth & Koushiappas 2011). An experiment aimed at direct search of NDM also fails to find it (Aprile & et al. 2011). The null results of the experiments could be reconciled with the amounts of dark matter ascertained through gravitational lensing at the scale of galaxy clusters. It is possible that the clustering scale of dark matter is larger, in which case dark matter would tend to clump around large clusters of galaxies rather than around separate galaxies.

## *Point mass approximation as a means to investigate motions in Galactic halo*

The asymptotic value of mass function of the Galactic gravitational potential (total Galaxy mass) can be obtained by investigating the motions of the most distant compact objects scattered in Galactic halo. They can be treated as test bodies moving in the background gravitational field. A primary quantity used to describe their motion in a statistical manner is the phase space distribution function. The radial velocity dispersion of halo objects and (normalized) number density are secondary quantities defined as appropriate integrals involving the phase space distribution function.

Mass density of matter producing gravitational field is not necessarily directly related to the radial velocity dispersion of test objects moving in that field. As an example of a system realized in nature for which this is true can be given the structure of Saturn

rings. The countless particles (of which the rings consist of) move as test bodies in the gravitational field of the planet and the rings do not contribute significantly to this field – the gravitational potential is unrelated to the density function of the rings in the Jeans equations.

It cannot be excluded the possibility that the heavy NDM halo is not present in the Galaxy and this hypothesis should be tested. In this case, at radii sufficiently large, the gravitational field would be approximately that of a point mass – the contribution to the gravitational field from higher multi-poles of the compact mass distribution (consisting of Galactic disk and a spheroidal component of which part is the central bulge and a halo of gas and stars) would only slightly affect orbits of external objects. These objects would not contribute significantly to that field and could be regarded as test bodies for which the Kepler problem applies with the central mass representing total Galaxy mass. Thus, when gravitationally bound to Galaxy, every compact object of the halo could be assumed to move in the asymptotic field as a test body on an elliptic orbit. One can study a collection of such orbits and calculate various expectation values over concentric spherical shells centered at the origin. It is evident that the radial velocity dispersion of the objects or the velocity dispersion anisotropy would not be directly related to the gravitating mass distribution – owing to the small number of halo objects they could be added or removed without changing the field, whereas the radial velocity dispersion profile could be changed significantly.

The idea of studying the motion of halo objects in the point mass approximation should not astonish, as it is not new. It was considered already 30 years ago by Bahcall & Tremaine (1981) and applied to several external galaxies. They proposed some estimators of galactic mass, all being an average of the quantity  $v_z^2 R/G$  over external halo objects, times a constant factor. The factor depended on the assumption about the mean square of eccentricity. A recent paper (Watkins et al. 2010) offers in essence the same method as originally proposed by Bahcall & Tremaine (1981). The difference is the presence of arbitrary power of distance in the mass estimators (owing to the assumptions about the spatial distribution of halo objects and the velocity dispersion anisotropy). Using estimators of this kind is tantamount to assuming a very special family of phase space distribution functions, which is a strong constraint. Interestingly, they found that the Galaxy mass could be as low as  $4 \times 10^{11} M_\odot$  (but, among tenths of other masses, they give also  $2.7 \times 10^{12} M_\odot$  as their preferred result if *Leo I* is assumed gravitationally bound to Galaxy).

Our approach to investigating the motion of halo objects in the point mass approximation is essentially different – it does involve estimators of this kind. We allow for arbitrary phase space distribution function, it is not a priori assumed. It is quite a generic function of two variables (energy and eccentricity) with the only assumption that the system is spherically symmetric. Expectation values of various characteristic quantities such as the dispersion tensor anisotropy, the profile of the radial velocity dispersion, all become functions of Galactocentric distance. In particular, we abandon the constraining assumption of setting the anisotropy parameter as a global constant. Our model allows for the possibility that on average the external orbits could be more elongated than internal ones. One of advantages is to avoid overestimation of Galaxy mass. We apply a minimizing scheme that enables to find the optimal form of the phase space function from the measurements of halo objects.

The result of the present work is to show that the observed motion of halo compact objects (like stars, satellite globular clusters or dwarf galaxies) can be made consistent with a low Galaxy

mass of about  $2.1 \times 10^{11} M_\odot$  at a distance 180 kpc, much lower than predicted by other models, and only  $\approx 7/5$  times greater than that predicted in the disk model framework based on the Galaxy rotation curve (extending out to 20 kpc). With this mass *Leo I* and *Hercules* cannot be gravitationally bound to Galaxy.

The paper is organized as follows. In the next section we give simple estimates for Galaxy mass. This will be similar to what other papers offer in the point mass approximation. The third section contains our general solution to Jeans equation in a point mass field for a general spherically symmetric collection of confocal orbits of test bodies moving in the space limited by two concentric spherical shells centered at the origin. This requires considering a finite support for the cutoff phase space distribution function and a related problem of choosing the appropriate set of independent variables on a fragment of a the plane of energy and eccentricity. Also some expectation values over thin spherical shells are defined which are indispensable in determining the mean values of various observables as functions of the galactocentric distance. In the fourth section we determine the radial velocity dispersion for compact objects in Galaxy halo, then we discuss briefly a minimizing scheme for finding the phase space distribution function in the framework of Keplerian ensemble, and finally we apply our method to find the Galaxy mass in the point mass approximation. Then we give conclusions.

Throughout this paper we assume the following parameters:  $R_s = 7.62 \pm 0.32$  kpc for Sun's distance from the Galactic center (Eisenhauer & et al 2005),  $V_s = 208 \pm 16$  km/s for the local disk rotation speed (Brainerd 2007) and  $\{U, V, W\} = \{9.96 \pm 0.33, 5.25 \pm 0.54, 7.07 \pm 0.34\}$  km/s for the components of the velocity vector of the Sun with respect to the local standard of rest (Aumer & Binney 2009) (for a summary of other measurements, see (Francis & Anderson 2009)).

## 2 SIMPLE ESTIMATES OF GALAXY MASS

In the case of spherical systems one can look for a relation  $M(r) = G^{-1} r \alpha(r) \langle v_r^2(r) \rangle$  between mass function  $M(r)$  and radial velocity dispersion function  $\langle v_r^2(r) \rangle$  determined over thin spherical shells. The coefficient  $\alpha(r)$  is a dimensionless function of galactocentric distance  $r$ . The connection between  $M(r)$  and  $\langle v_r^2(r) \rangle$  is model-dependent and the predicted asymptotic mass can be different for the same halo measurements.

The assumed mass function in NDM halo models is related to the theoretical  $\langle v_r^2(r) \rangle$  profile through Jeans and Poisson equations. There is no freedom in modifying the phase space distribution function (modulo free parameters) since it is assumed. The free parameters are found by minimizing a measure of distance between  $\langle v_r^2(r) \rangle$  and halo measurements. The parameters, and so the total mass, are not uniquely determined, the same dispersion profiles could be explained by models with different total masses (this is the mass-anisotropy degeneracy). In the case of a point mass source, the coupling function  $\alpha(r)$  is a functional of eccentricity and energy over various orbits of test bodies, whereas  $M(r)$  is constant. There are possible infinitely many functions  $\langle v_r^2(r) \rangle$  in the same gravitational field. This freedom would be limited by imposing an ansatz for the number density of compact halo objects, or by assuming the dispersion anisotropy parameter as constant, etc. Starting from section 3 onwards, we will refrain from making such constraining assumptions.

## 2.1 Galaxy mass from escape velocity

At distances from the Galactic center sufficiently large, the gravitational field can be approximated by that of a point mass  $M$  located at the center and regarded as the total gravitating mass of Galaxy. For a distant test body bound in such a field

$$\frac{r\dot{r}^2}{2GM} = 1 - \frac{J^2}{2GMr} + \frac{Er}{GM} < 1 - \sqrt{1 - e^2} < 1.$$

Here,  $0 \leq e < 1$  is the eccentricity of an elliptical orbit,  $E$  and  $J$  are the energy and angular momentum (per unit mass), and

$$1 + \frac{2EJ^2}{G^2M^2} = e^2, \quad 0 > E \geq -\frac{G^2M^2}{2J^2}.$$

Hence, there is an upper bound for the absolute value of  $V_r \equiv \dot{r}$  possible for a remote halo object,  $V_r^2 < \frac{2GM}{r}$ , provided the object is gravitationally bound. One can try to estimate the lower bound for the Galactic mass by inverting the inequality. This gives us the escape mass observable in spherical symmetry

$$\mathcal{M}(r) = \frac{rV_r^2(r)}{2G} < M.$$

A histogram showing the number of catalogued halo objects with  $\mathcal{M}$  not greater than some limit is presented in figure 1.

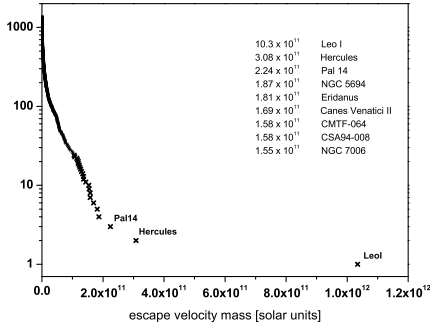


**Figure 1.** Escape mass histogram for halo objects. It shows the number of objects with  $\frac{rV_r^2(r)}{2G}$  not greater than a given value (in solar units).

Among halo objects there can be some that are not gravitationally bound to Galaxy and should be excluded from the analysis. *Leo I* with the highest  $\mathcal{M} = 10.3 \times 10^{11} M_\odot$  is such an object (this will be justified later). As so, the estimate for the Galaxy mass is  $3 \times 10^{11} M_\odot$  at  $R \approx 130$  kpc, provided that *Hercules* is bound to Galaxy on almost radial orbit. This value is to be compared with the integrated Galaxy dynamical mass of  $1.44 \times 10^{11} M_\odot$  at  $R \approx 20$  kpc predicted in the global disk model (Jalocha et al. 2010) for the rotation curve shown in Fig. 2. This value is smaller than that for a spherically symmetric mass model in Fig. 3 which gives the dynamical mass estimate of about  $2.0 \times 10^{11} M_\odot$  at  $R \approx 20$  kpc. The lower bound for total Galaxy mass at  $R \approx 20$  kpc can be something in between  $2 \times 10^{11} M_\odot$  and  $3 \times 10^{11} M_\odot$ . Then only  $\approx 30\%$  of the total Galaxy mass would reside outside  $R = 20$  kpc.

## 2.2 A simple mass estimate from Jeans theory

For a spherically symmetric system in a steady state with vanishing mean velocities

$$\frac{r\rho_{,r}}{\rho} + 2\beta = -\frac{r}{\langle v_r^2 \rangle} \left( \Phi + \langle v_r^2 \rangle \right)_{,r}, \quad \beta = 1 - \frac{\langle v_\theta^2 \rangle + \langle v_\phi^2 \rangle}{2\langle v_r^2 \rangle}$$

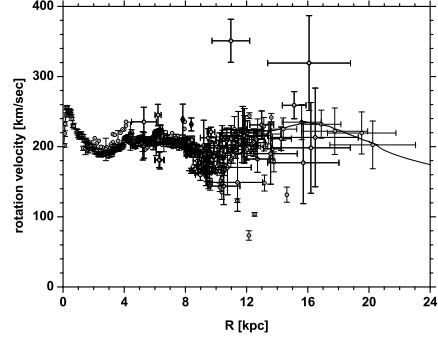


**Figure 2.** Galaxy rotation curve. A unified rotation curve from (Sofue et al. 2009) prepared at  $R_S = 200$  kpc and  $V_S = 200$  km/s [circles+error bars] and their model rotation curve (Honma & Sofue 1996) [solid thick line]. The extended rotation curve in disk model [thin solid line]

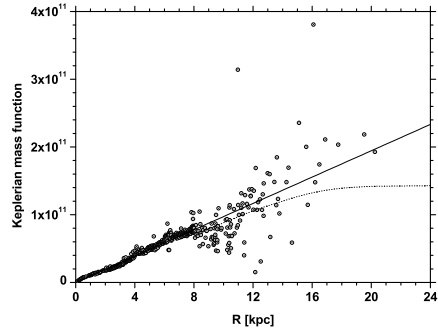


**Figure 3.** Keplerian mass function  $rv_\phi^2/G$  for Galaxy rotation data [circles] and a linear fit  $M(r) = 9.72 \times 10^9 R$  [solid line]. To compare with, the disk model mass function has been also shown [dotted line].

from Jeans equations. On assuming that  $\langle v_r^2 \rangle$  is almost constant at radii sufficiently large, that the transverse and radial dispersions are proportional to each other so that  $\beta$  is constant, that  $r\Phi \sim -GM$  and  $\rho \sim \rho_o (r_o/r)^{3+\varepsilon}$  (with small  $\varepsilon > 0$  to ensure integrability at infinity), then  $\alpha r \langle v_r^2 \rangle \sim GM$  if  $\alpha = 4 + \varepsilon - 2\beta$ . We see that  $M$  can be made arbitrarily large if the velocity ellipsoid is sufficiently flat ( $\beta \ll 0$ ). A reasonable assumption for the simple model is a marginally integrable halo ( $\varepsilon = 0^+$ ) with isotropic velocity dispersion ( $\beta \approx 0$ ), then  $\alpha(r) \approx 4$ :

$$M = \frac{4r}{G} \langle v_r^2 \rangle.$$

By applying this "flat" model outside  $r = 30$  kpc to the (asymptotically nonconstant) dispersion profiles we present later (see Fig. 11), one can obtain the following estimate for Galactic mass:  $5.4 \times 10^{11} M_\odot$  if we discard *Leo I*;  $4.4 \times 10^{11} M_\odot$  if we discard *Leo I* and *Hercules*; and  $4.0 \times 10^{11} M_\odot$  if we discard *Leo I*, *Hercules* and *Pal 14*.

Corresponding to the above model is the following mass estimator  $M = \frac{4}{GN} \sum_i r_i v_{r,i}^2$  using a number of  $N$  outermost halo objects. A similar class of estimators in the point mass approximation was considered in (Bahcall & Tremaine 1981). The result is shown in Fig. 4 as function of the number of most distant objects, assuming that *Leo I* is not bound to Galaxy. The function has a distinct minimum and a following maximum in which region the num-

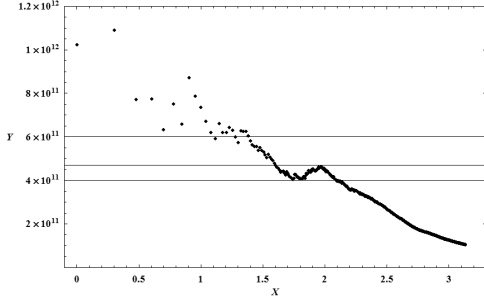


**Figure 4.** The result of applying the estimator of total mass  $\mathcal{M}_N = \frac{4}{GN} \sum_{i=1}^N r_i v_{r_i}^2$  to outermost  $N$  compact objects in Galactic halo shown as a function of  $N$ .  $X = \log_{10} N$ ,  $Y = \mathcal{M}_N / M_\odot$ . *Leo I* is excluded from the analysis. The most distant object is *Leo T* at  $r = 417$  kpc with  $rv_r^2/G \approx 2.5 \times 10^{11} M_\odot$ .

ber of objects grows from a dozen to a hundred without a significant change in the estimated mass. The maximum  $4.6 \times 10^{11} M_\odot$  can be taken as a safe mass estimate. As it is seen from the diagram, the same value of mass could be obtained by taking into account only 41 most distant objects, with the one closest to the center located at  $\approx 46.1$  kpc. A similar analysis with the exclusion of *Leo I* and *Hercules* gives  $4.4 \times 10^{11} M_\odot$  with 37 objects outside 46.7 kpc, and with the exclusion of *Leo I*, *Hercules* and *Pal 14* gives  $4.3 \times 10^{11} M_\odot$  with 26 objects outside 50.9 kpc. With such masses both *Hercules* and *Pal 14* with escape mass  $2.95 \times 10^{11} M_\odot$  and  $2.12 \times 10^{11} M_\odot$ , respectively, could be bound to Galaxy. (To compare with, for the sample of halo objects studied in (Watkins et al. 2010) the mass estimate would be  $5.5 \times 10^{11} M_\odot$  without *Leo I* which compares to our  $4.6 \times 10^{11} M_\odot$ ; or  $8.5 \times 10^{11} M_\odot$  with *Leo I* included – in either case *Leo I* could not be bound to Galaxy).

The conclusion is that high Galaxy mass estimates come from large values of the theoretical coefficient  $\alpha$ , depending on models. As seen from table 1, the coefficient could be increased by a factor of 1.25 by assuming phase space distribution function  $f(e, \epsilon) = \epsilon^{5/2}$  (with constant anisotropy  $\beta = -1$ ). This way Galaxy mass could be increased without limits. Our goal is quite opposite, we aim to reduce  $\alpha(r)$  to a minimum admissible by the observational data using a model maximally flexible with the minimum number of assumptions. This cannot be achieved using simple models with constant  $\beta$ .

### 2.3 A hindsight for mass observable

The time average of  $rv_r^2$  over an elliptical orbit with eccentricity  $e$  is proportional to the central mass  $M$ :  $\frac{2}{e^2} \langle \frac{rv_r^2}{G} \rangle_t = M$ , similarly,  $\frac{1}{1-e^2} \langle \frac{rv_\phi^2}{G} \rangle_t = M$ . These two averages are equal when  $e^2 = 2/3$ , in which case  $M = 3 \langle \frac{rv_r^2}{G} \rangle_t$ . Analogously, for equal mean values of  $v_r^2$  and  $v_\phi^2$  in the plane of motion,  $1 = \frac{\langle v_\phi^2 \rangle_t}{\langle v_r^2 \rangle_t} = \frac{1-e^2+\sqrt{1-e^2}}{e^2}$ , hence  $e^2 = \frac{3}{4}$  and  $\frac{8}{3} \langle \frac{rv_r^2}{G} \rangle_t = M$ . With this hindsight, we choose an observable which best suits our task at hand. This must be some average of  $rv_r^2$ . For a collection of orbits, the mean value of  $\langle rv_r^2 \rangle_t$  can be determined knowing the number of orbits with particular energy and eccentricity. In the next section we shall deal with averaging over concentric spherical surfaces.

### 3 SPHERICALLY SYMMETRIC ENSEMBLE OF TEST BODIES IN THE FIELD OF A POINT MASS

The motion of a test body in a spherically symmetric potential  $\Phi(r)$  is planar in a plane through the origin. The plane is determined by two integrals of motion – a unit normal to the plane. The additional two integrals of motion are energy  $E$  and magnitude of angular momentum  $J$  (both per unit mass). In terms of angular velocity  $\omega$ ,  $\omega^2 = \dot{\theta}^2 + \dot{\phi}^2 \sin^2 \theta$ , the two integrals read

$$r^2 \omega^2 = \frac{J^2}{r^2}, \quad v_r^2 = 2E - 2\Phi - \frac{J^2}{r^2}.$$

In the particular case of Newtonian potential

$$\Phi = -\frac{GM}{r},$$

there is an additional integral of motion indicating a fixed direction in the plane of motion.

The condition  $v_r^2 \geq 0$  for all  $r > 0$  with  $J \neq 0$  gives  $1 + \frac{2EJ^2}{G^2M^2} \geq 0$ . We are interested only in spatially bound orbits. Two turning points will be possible (or  $v_r \equiv 0$ ) when  $E < 0$  and  $1 + \frac{2EJ^2}{G^2M^2} < 1$ . Hence, elliptical orbits are possible only for pairs  $(E, J)$  such that  $0 \leq 1 + \frac{2EJ^2}{G^2M^2} < 1$ . Elliptical motion can be thus uniquely determined by specifying five numbers: three Euler angles describing orientation of the orbit in space and a pair of numbers  $(e, \epsilon)$  defined by

$$e = \sqrt{1 + \frac{2EJ^2}{G^2M^2}}, \quad 0 \leq e < 1, \quad \epsilon = -\frac{RE}{GM} > 0.$$

Here,  $R$  is some unit of length,  $e$  is the eccentricity and  $\epsilon$  is a measure of energy determining the length of the large semiaxis, which is  $\frac{R}{2\epsilon}$ . The turning points are  $\frac{R}{2\epsilon}(1 \pm e)$ . The dimensionless parameters  $(e, \epsilon)$  play the central role in further considerations.

To find various expectation values for a spherically symmetric collection of confocal ellipses, it suffices to know a distribution function describing the number of ellipses of a given eccentricity  $e$  and energy  $-\epsilon$ . It will be related to the distribution function  $f(\vec{r}, \vec{v})$  in the  $\mu$ -phase space. We assume that  $f$  can be expressed through first integrals  $e$  and  $\epsilon$ . Then,  $f$  is stationary and satisfies the necessary condition  $\partial_t f + \partial_{q^i} f + \partial_{q^i} f \partial^i \Phi = 0$  for a distribution of a collisionless system. This is the wording of the Jeans theorem in our situation.

As an example, consider an almost axisymmetric collection of confocal ellipses randomly distributed in a plane (see Fig. 5). One can assign to it a substitute smooth density function describing the expected number of bodies in a given surface element, assuming that every ellipse corresponds to a single body. In finding the density one should take into account the fact that the probability of finding a body at a given point on its trajectory is proportional to the fraction of time spent in a given arc element. Given a family of orbits one can calculate expectation values for various observables at some distance from the center by taking into account the number of various ellipses crossing a circle concentric with the origin, which all become functions of the circle's radius. The most important observables are: the radial velocity dispersion, the mean eccentricity of orbits intersecting that circle, or the mean value of the velocity anisotropy parameter. Similarly, one can consider a spherically symmetric collection of confocal ellipses in space, which is the subject of the next section.

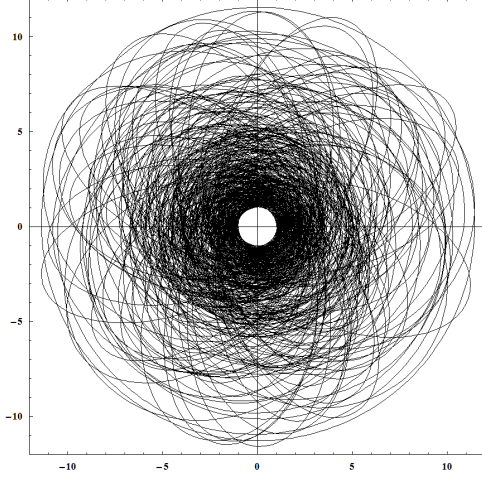


**Figure 5.** A random collection of confocal ellipses in a plane generated so as all ellipses are entirely contained within some annulus (here  $1 < r < 12$ ) with uniform probability for all admissible pairs  $(e, \epsilon)$ .

### 3.1 Expectation values for Keplerian ensemble

The integrals of motion  $e$  and  $\epsilon$  can be treated as new independent phase space variables. By making a transformation from ordinary spherical coordinates  $r, \theta, \phi, v_r, v_\theta, v_\phi$  to new coordinates  $u, \theta, \phi, \epsilon, e, \psi$  of the form

$$r \rightarrow Ru, \quad v_r^2 \rightarrow \frac{GM}{R} \left( \frac{2}{u} - \frac{1-e^2}{2\epsilon} \frac{1}{u^2} - 2\epsilon \right),$$

$$(\theta, \phi) \rightarrow (\theta, \phi), \quad (v_\theta, v_\phi) \rightarrow \sqrt{\frac{GM}{R}} \frac{\sqrt{1-e^2}}{u} (\sin \psi, \cos \psi),$$

the original volume element  $r^2 dr \wedge \sin \theta d\theta \wedge d\phi \wedge 2 \frac{dv_r^2}{2v_r} \wedge dv_\theta \wedge dv_\phi$  (factor 2 to account for two signs of  $v_r$ ) is transformed (up to a constant factor) to

$$\frac{du \wedge \sin \theta d\theta \wedge d\phi \wedge d\psi \wedge d\epsilon \wedge e de}{\sqrt{\epsilon \left( \epsilon - \frac{1-e}{2u} \right) \left( \frac{1+e}{2u} - \epsilon \right)}}.$$

For we have already assumed spherical symmetry, the angles  $\phi, \theta$  and  $\psi$  can be integrated out. The form of the volume element defines the integration region.

In finding expectation values as function of radial distance, integration must be carried out over all ellipses intersecting a spherical thin shell of some fixed radius  $r$  centered at the origin. Given  $0 < r < \infty$  and  $0 \leq e < 1$ , we have  $\frac{1-e}{2u} \leq \epsilon \leq \frac{1+e}{2u}$  for such orbits. Hence, we arrive at the distribution integral

$$\int f(\vec{r}, \vec{v}) d^3 \vec{r} d^3 \vec{v} \propto \int_0^\infty du \nu_u[f]$$

where

$$\nu_u[f] = \int_0^1 e de \int_{\frac{1-e}{2u}}^{\frac{1+e}{2u}} d\epsilon \frac{f(e, \epsilon)}{\sqrt{\epsilon \left( \epsilon - \frac{1-e}{2u} \right) \left( \frac{1+e}{2u} - \epsilon \right)}}.$$

For physical reasons, it is convenient to assume that all orbits of the ensemble are contained entirely within a spherical annulus  $Ru_a < r < Ru_b$  (in between two limiting spheres of radius  $r_a = Ru_a$  and  $r_b = Ru_b$ ). This requirement imposes restrictions on the integration region in the phase space, changing considerably the support of  $f(e, \epsilon)$ . Then,  $u_a < \frac{1-e}{2\epsilon}$  and  $\frac{1+e}{2\epsilon} < u_b$ . Hence,

$\frac{1+e}{2u_b} < \epsilon < \frac{1-e}{2u_a}$  and thus also  $0 \leq e < \frac{u_b - u_a}{u_b + u_a} < 1$ . As a result, the integration region has been shrunk to a quadrilateral **abcB** as shown in figure 6. However, integration requires splitting of the

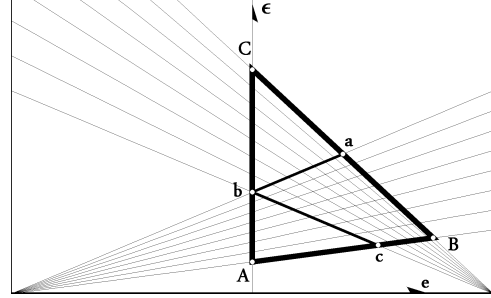


**Figure 6.** The points on the plane  $(e, \epsilon)$  represent confocal elliptical orbits of eccentricity  $e$  and energy  $-\epsilon$ . The **ABC** triangle with vertices **A**  $(0, \frac{1}{2u_b})$ , **B**  $(\frac{u_b-u_a}{u_b+u_a}, \frac{1}{u_a+u_b})$ , **C**  $(0, \frac{1}{2u_a})$  comprises all orbits contained entirely between two spheres of radii  $u_a$  and  $u_b$  and centered at the focal point. The two families of lines  $\epsilon = \frac{1+e}{2u} \alpha$  through point  $(-1, 0)$  and  $\epsilon = \frac{1-e}{2u} \beta$  through point  $(1, 0)$  cross with each other forming a new coordinate system  $(\alpha, \beta)$  on the plane  $(e, \epsilon)$ . When  $\alpha \in (\frac{u}{u_b}, 1)$  and  $\beta \in (1, \frac{u}{u_a})$  the coordinates cover only a quadrilateral **abcB** with vertices **a**  $(\frac{u-u_a}{u+u_a}, \frac{1}{u+u_a})$ , **b**  $(0, \frac{1}{2u})$ , **c**  $(\frac{u_b-u}{u_b+u}, \frac{1}{u_b+u})$  and **B** as required. Quadrilateral **abcB** is the locus of all orbits  $(e, \epsilon)$  which cross a sphere of some radius  $u_a < u < u_b$  at least once.

$u$ -dependent integration region into three parts. To overcome this difficulty we introduce a mapping  $(\alpha, \beta) \rightarrow (e(\alpha, \beta), \epsilon_u(\alpha, \beta))$  from a rectilinear region with cartesian coordinates  $(\alpha, \beta)$  to a  $u$ -dependent irregular region **abcB**. This leads to the following coordinate change in the reduced phase space  $(\epsilon, e, u)$  in integral  $\nu_u[f]$ :

$$e \rightarrow e(\alpha, \beta) = \frac{\beta - \alpha}{\beta + \alpha}, \quad \epsilon \rightarrow \epsilon_u(\alpha, \beta) = \frac{1}{u} \frac{\alpha \beta}{\alpha + \beta}, \quad u \rightarrow u,$$

$$\frac{u_b}{u_b} < \alpha < 1, \quad 1 < \beta < \frac{u}{u_a}, \quad 0 < u_a < u < u_b.$$

The interpretation and the origin of this coordinate change is depicted in figure 6. We get finally,

$$\int f(\vec{r}, \vec{v}) d^3 \vec{r} d^3 \vec{v} \propto \int_{u_a}^{u_b} du \sqrt{u} \mu_u[f],$$

where

$$\mu_u[f] = \int_{u/u_b}^1 \frac{d\alpha}{\sqrt{1-\alpha}} \int_1^{u/u_a} \frac{d\beta}{\sqrt{\beta-1}} \frac{\beta - \alpha}{(\alpha + \beta)^{5/2}} f\left(\frac{\beta - \alpha}{\beta + \alpha}, \frac{1}{u} \frac{\alpha \beta}{\alpha + \beta}\right).$$

Now, given  $f(e, \epsilon)$ , all expectation values can be in principle determined. In calculating them the following expressions will be useful

$$\frac{rv_r^2}{GM} = 2 \frac{(1-\alpha)(\beta-1)}{\alpha+\beta}, \quad \frac{rv_\phi^2}{GM} = \frac{2}{\alpha+\beta}, \quad e = \frac{\beta - \alpha}{\beta + \alpha}.$$

For the purpose of further applications the most important are averages over concentric thin spherical shells. The mean value of a function  $g$  defined on a spherical shell of radius  $r$  is

$$\langle g \rangle_r = \frac{\mu_u[f g]}{\mu_u[f]}.$$

The above expression for  $\langle g \rangle_r$  is quite analogous to a conditional probability 'A provided that B'. Consequently, the average over all spherical shells can be calculated from

$$\langle g \rangle = \frac{\int du \langle g \rangle_u \mu_u[f]}{\int du \mu_u[f]}.$$

As a simple example, consider  $f(e, \epsilon) = C\epsilon^{3/2}$  in the limit  $u_a \rightarrow 0$ ,  $u_b \rightarrow \infty$ . Then,  $\frac{\langle rv_r^2 \rangle_r}{GM} = \frac{1}{4}$ , the number density must behave as  $r^{-3}$  (the number of particles diverges logarithmically). With the same function  $f$  but with different support so that all orbits with  $u < u_a = 1/24$  or  $u > u_b = 24$  were not present in the system, the density profile and averages change considerably (see Fig. 7). See also table 1 and figure Fig. 8 for various other  $f$ 's.

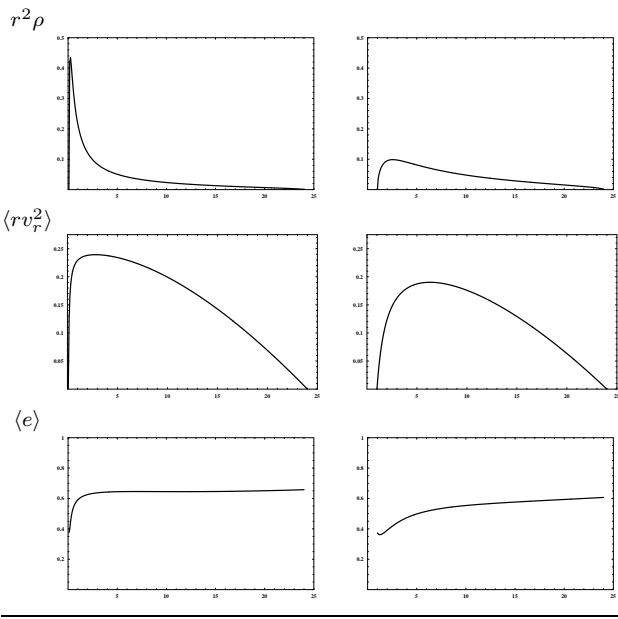


**Figure 7.** Various observables averaged over spherical surfaces shown as functions of the spherical radius with phase space distribution function  $f(\epsilon, e) \propto \epsilon^{3/2}$ . The expectation value for the density of objects  $\rho$  is integrable to unity. First column shows expectation values with the support  $1/12 < u < 24$  and the second column with  $1 < u < 24$ .

The lesson we gain is that in the halo modeling we should assume  $f \sim \epsilon^{3/2+\delta}$  as  $\epsilon \rightarrow 0$ ,  $\delta > 0$  (for integrable number density). In addition, we can assume  $u_a > 0$  to eliminate all orbits with pericenter smaller than  $u_a$ . Physically, this condition allows for considering only bodies moving sufficiently far from the center. In conjunction with the previous condition, the number density will be globally integrable. The former condition can be released by considering orbits for which  $u < u_b$  always. Then, the cumulative number of objects will start from zero at  $u = u_a$  and grow until it saturates at  $u = u_b$ .

#### 4 APPLICATION TO GALACTIC HALO

We will be using averages  $\langle rv_r^2 \rangle / G$  over (reasonably thin) concentric spherical shells as the basic observable. It is the simplest one with the dimension of mass formed out of pairs  $(r, v_r)$  measurable for halo objects. It resembles a size independent time average for a single closed orbit  $\langle rv_r^2 \rangle_t = \frac{1}{2} GM e^2$ . In order that  $\langle rv_r^2 \rangle$  could be determined from measurements as a function of  $r$  with a satisfactory resolution, a reasonable number of compact objects in Galaxy halo is needed in every of a number of sufficiently thin concentric spherical shells centered at the origin.

To prepare the  $\langle rv_r^2 \rangle / G$  profile we used position-velocity data from the following papers: Clewley et al. (2004); Mateo

| $f(e, \epsilon)$     | $r^2 \rho$    | $\frac{\langle rv_r^2 \rangle}{GM}$ | $\frac{\langle rv_\phi^2 \rangle}{GM}$ | $\beta$          | $\langle e \rangle$ | $\langle e^2 \rangle$ |
|----------------------|---------------|-------------------------------------|--|------------------|---------------------|-----------------------|
| $\epsilon^{1/2}$     | $\sim r^0$    | $\frac{1}{3}$                       | $\frac{2}{3}$                          | -1               | $\frac{2}{3}$       | $\frac{1}{2}$         |
| $\epsilon^{1/2} e^2$ | $\sim r^0$    | $\frac{7}{15}$                      | $\frac{8}{15}$                         | $-\frac{1}{7}$   | $\frac{4}{5}$       | $\frac{2}{3}$         |
| $\epsilon^{1/2} e^4$ | $\sim r^0$    | $\frac{19}{35}$                     | $\frac{16}{35}$                        | $\frac{3}{19}$   | $\frac{6}{7}$       | $\frac{3}{4}$         |
| $\epsilon^{1/2} e^6$ | $\sim r^0$    | $\frac{187}{315}$                   | $\frac{128}{315}$                      | $\frac{59}{187}$ | $\frac{8}{9}$       | $\frac{4}{5}$         |
| $\epsilon^{3/2}$     | $\sim r^{-1}$ | $\frac{1}{4}$                       | $\frac{1}{2}$                          | -1               | $\frac{2}{3}$       | $\frac{1}{2}$         |
| $\epsilon^{3/2} e^2$ | $\sim r^{-1}$ | $\frac{1}{3}$                       | $\frac{1}{3}$                          | 0                | $\frac{4}{5}$       | $\frac{2}{3}$         |
| $\epsilon^{3/2} e^4$ | $\sim r^{-1}$ | $\frac{3}{8}$                       | $\frac{1}{4}$                          | $\frac{1}{3}$    | $\frac{6}{7}$       | $\frac{3}{4}$         |
| $\epsilon^{3/2} e^6$ | $\sim r^{-1}$ | $\frac{2}{5}$                       | $\frac{1}{5}$                          | $\frac{1}{2}$    | $\frac{8}{9}$       | $\frac{4}{5}$         |
| $\epsilon^{5/2}$     | $\sim r^{-2}$ | $\frac{1}{5}$                       | $\frac{2}{5}$                          | -1               | $\frac{52}{75}$     | $\frac{8}{15}$        |
| $\epsilon^{5/2} e^2$ | $\sim r^{-2}$ | $\frac{1}{4}$                       | $\frac{1}{4}$                          | 0                | $\frac{57}{70}$     | $\frac{11}{16}$       |
| $\epsilon^{5/2} e^4$ | $\sim r^{-2}$ | $\frac{3}{11}$                      | $\frac{2}{11}$                         | $\frac{1}{3}$    | $\frac{200}{231}$   | $\frac{42}{55}$       |
| $\epsilon^{5/2} e^6$ | $\sim r^{-2}$ | $\frac{2}{7}$                       | $\frac{1}{7}$                          | $\frac{1}{2}$    | $\frac{620}{693}$   | $\frac{17}{21}$       |

**Table 1.** Averages over an infinitesimally thin spherical shell of radius  $r$  for a spherically symmetric ensemble of confocal elliptical orbits described by phase space distribution function  $f(e, \epsilon)$ . These values are only for illustration (the number density  $\rho$  of test bodies is nonintegrable). Parameter  $\beta$  is the anisotropy parameter of the velocity ellipsoid. With these simple  $f(e, \epsilon)$ 's all the quantities (except  $\rho$ ) are independent of  $r$ .

(1998); Wilhelm et al. (1999); Starkenburg et al. (2009); Dohm-Palmer et al. (2001); Harris (1996) and recalculated to epoch J2000 when necessary. In addition, we included objects like *Ursa Major I* and *II*, *Leo IV*, *Leo T*, *Coma Berenices*, *Canes Venatici I* and *II*, *Hercules* (Simon & Geha 2007), *Bootes I*, *Willman I* (Martin et al. 2007), *Bootes II* (Koch et al. 2009), *Leo V* (Belokurov et al. 2008), *Segue I* (Geha et al. 2009), and *Segue II* (Belokurov et al. 2009). In total, we used 1361 compact objects in our sample.

The sample of halo objects is shown on the  $(r, rv_r^2/G)$  plane in Fig. 9. It is not representative and is insufficient to determine a reliable profile of  $\langle rv_r^2 \rangle$  at larger radii. Most of objects are located in the Sun vicinity along a few directions only and the statistics is very poor at the most crucial for Galaxy mass determination region of the outermost radii where only several objects are present spread over a wide interval of Galactocentric radius, see Fig. 10. The problem of lacking data will affect the accuracy of determination of the phase space distribution function which is the basis of the statistical treatment of halo objects. Owing to the small number of objects, we will have to assess the influence of the choice of halo objects on the accuracy of determination of the  $\langle rv_r^2 \rangle$  profile – there can be still objects that are not included in the catalogue and their addition could change the results. To mimic this situation, we will superpose  $\langle rv_r^2 \rangle$  profiles prepared for random sub-samples of the existing catalogue.

##### 4.1 The $\langle rv_r^2 \rangle$ profile for compact objects in Galactic halo

We excluded from the analysis *Leo I* with escape mass  $> 10^{12} M_\odot$ . The high speed of *Leo I* might be due to a three-body ejection mechanism as noted by Sales et al. (2007), the same remark could be applied to some of the fast-receding satellites. Assuming that *Leo I* was gravitationally bound to Galaxy would make the whole

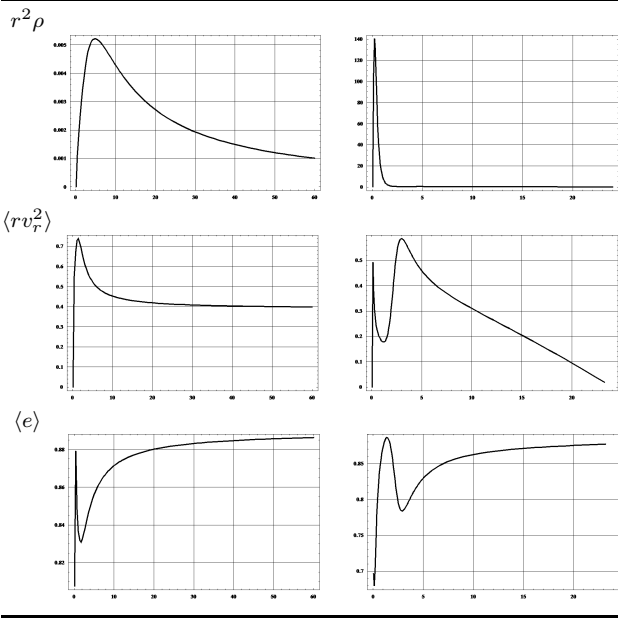


**Figure 8.** Various observables averaged over spherical shells as functions of spherical radius. First column for  $f(e, \epsilon) \propto e^5 \epsilon^{3/2+1/12} (e^{1/8} - e\epsilon)^8$  with support  $1/12 < u < \infty$ . Second column for  $f(e, \epsilon) = \left( (1 - 2e^2)^2 + 144e^6 \epsilon^{1/6} \right) \epsilon^{5/3} (1 - 4e^2 \epsilon)^2$  and support  $1/24 < u < 24$ .

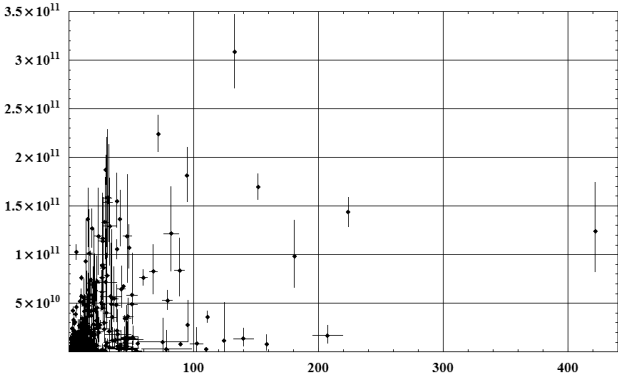


**Figure 9.** Halo objects in the  $(r, \frac{1}{2}rv_r^2/G)$  plane. The values show minimal mass required to gravitationally bind a particular halo object. The only object not shown is *Leo I* for which  $\frac{1}{2G}rv_r^2 = 1.03 \times 10^{12} M_\odot$  (at  $r = 254 \text{ kpc}$ ).

work of inferring Galaxy mass from Jeans theory meaningless as then Galaxy mass could be decided to be not lower than  $10^{12} M_\odot$  based on a single measurement, regardless of what value indicated the motion of tenths of other objects. As to another object *Leo T*, it cannot be included in preparing the  $\langle rv_r^2 \rangle$  profile owing to the fact that it is isolated from other objects on the axis of galactocentric distance (one cannot calculate dispersion for a single element). This fact will not reduce the Galaxy mass estimate due to moderate value of escape mass for *Leo T* which is  $1.24 \times 10^{11}$ . The remaining objects were used to find the  $\langle rv_r^2 \rangle$  profile as described below.

To determine function  $\langle rv_r^2 \rangle$  and see how the choice of objects could influence it, we chose 7001 subsamples, each consisting of randomly chosen  $\sim 2/3$  of the totality of objects. A particular subsample was an ordered list of pairs  $(r, rv_r^2)$ . Each of these lists

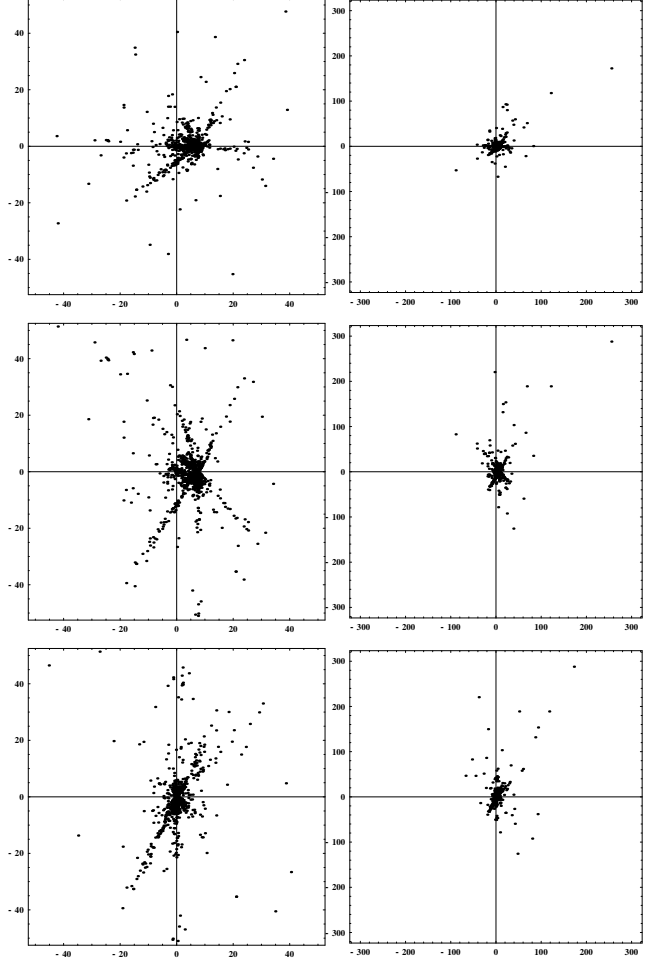


**Figure 10.** Distribution of halo objects in space: projection onto the XY plane (the Galactic plane) [top], projection onto the XZ plane [middle], and projection onto the YZ plane [bottom].

was split into sublists of equal length  $k$  called  $k$ -boxes. A  $k$ -box contained objects with similar galactocentric distance. The mean values  $(\langle r \rangle, \langle rv_r^2 \rangle)$  were calculated for every  $k$ -box in a list. The  $k$  could be chosen small without affecting the reliability of finding  $\langle rv_r^2 \rangle$  at smaller radii where the concentration of halo objects was large – there were hundredths of such  $k$ -tuples at comparable mean radii. Averaging over these  $k$ -tuples would give correct result, the same as if obtained with a much greater  $k$ . Taking small  $k$  was justified by the fact there was only a few of catalogued objects at large radii – too large  $k$  would require calculating dispersion for a  $k$ -tuple containing halo objects with unacceptably large radial spread. We found  $k = 6$  to be optimal (we used also other  $k$ 's to compare with). Next, all the lists of averages were joined to form a single output list (for  $k = 6$  it consisted of  $\sim 10^6$  pairs  $(\langle r \rangle, \langle rv_r^2 \rangle)$  – a cloud of points on the  $(r, rv_r^2)$  plane). Then, the list was sorted according to increasing radii and converted to a shorter list with the help of a smoothing procedure with a fixed width window (we used 8kpc for the width). The data embraced by the window were averaged using a Gaussian filter (we assumed the window size to have been 4 times greater than the  $\sigma$  parameter in the Gaussian function). In effect, we obtained the required velocity dispersion profile  $\langle rv_r^2 \rangle$  as a function of  $r$ . It could have occurred that several identical  $k$ -tuples appeared in the output list, especially at larger radii, where the number of objects was small. Such a  $k$ -tuple was more frequent and effectively



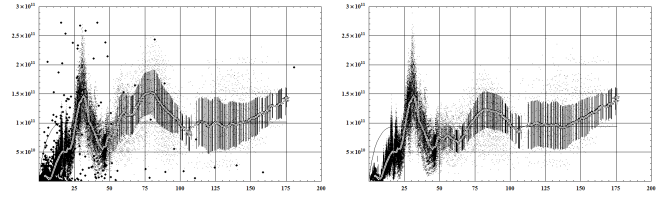
it entered with a greater weight into the average. It could have also happened that some  $k$ -tuples comprised objects with radii very different from each other, but this situation was rare at lower radii and would not affect the final result of the scanning procedure. It was more frequent only in the remotest region where the number of objects was small. A standard deviation from the mean was used as a measure of the uncertainty of determining function  $\langle rv_r^2 \rangle$ . The discussed box-sampling had also the advantage that the effective radial window size adapted automatically. For all  $k$ -tuples with the mean radii embraced by the scanning window, we obtained some effective window width changing smoothly with radius depending on the average radial spread of objects in a given  $k$ -box.

The result of the averaging procedure is shown in figure Fig. 11 for several choices of  $k$ . It is seen that  $\langle rv_r^2 \rangle$  is independent of  $k$  for small radii and it changes with  $k$  for larger radii. Function  $\langle rv_r^2 \rangle$  is thus reliable at lower radii where the number of objects per distance is high and it is much less reliable at the outermost radii where only a few objects are present scattered over a very large interval of distances. This is the nature of the measurement data and the situation cannot be improved unless new halo objects are found. By comparing with the isotropic model  $4\langle rv_r^2 \rangle/G$  discussed in section 2.2, we conclude that estimates of asymptotic mass will be sensitive to the assumptions made about which objects are not gravitationally bound to Galaxy. With only *Leo I* and *Hercules* considered as unbound, one can expect the mass to be 1.25 times greater than that obtained when, in addition to *Leo I* and *Hercules*, also *Pal 14* is assumed unbound. Mass estimates can change also depending on  $k$  by less than 10%.

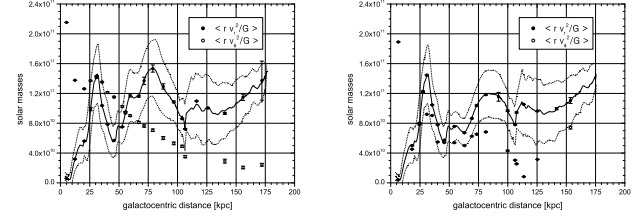
#### 4.2 Galaxy mass in the point mass approximation and a systematic way of obtaining the corresponding phase space distribution function

Function  $\langle rv_r^2 \rangle$  is a functional of phase space distribution function  $f(e, \epsilon)$ . Function  $f$  is defined on a triangular support (call it  $S$ ) as shown in figure Fig. 6, but only a fragment of it, an  $r$ -dependent rectangular region (call it  $S_r$ ) is used to find  $\langle rv_r^2 \rangle$  at a given radius  $r$ . Function  $f$  is not known in advance, it must be found based on  $\langle rv_r^2 \rangle$  known from observations. This task can be solved in many ways. Since  $f$  must be nonnegative, it can be expressed in terms of an auxiliary function  $h(e, \epsilon)$  so that  $f \equiv h^2 > 0$ . A possible idea to find  $f$  is to decompose  $h$  in a series of orthogonal functions on  $S$ . In a first approximation, only several first terms can be taken into account. Given a set of expansion coefficients, the corresponding  $\langle rv_r^2 \rangle$  can be calculated by numerical integration over  $S_r$  and compared with the observed  $\langle rv_r^2 \rangle$  profile. A norm of the difference between the theoretical and observed profiles  $\langle rv_r^2 \rangle$  gives rise to some error function of the unknown expansion coefficients. The optimal set of the coefficients can be found by minimizing the error function. A detailed description of the minimizing scheme can be found in Bratek et al. (2012). In finding  $f$  we assumed the radius of the internal boundary sphere as small as possible:  $r_a \approx 4\text{kpc}$ , and we verified that the mass is not sensitive to this choice as far as  $r_a < 24\text{kpc}$ . The radius of the external boundary sphere was set equal to the endpoint of the observed  $\langle rv_r^2 \rangle$  profile:  $r_b \approx 180\text{kpc}$ .

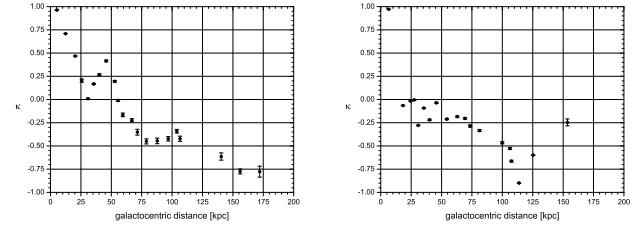
The results of applying the Keplerian ensemble method to the measurements of compact objects in Galactic halo (using the minimizing scheme) is shown and described in Fig. 12. Assuming that *Leo I* and *Hercules* are not gravitationally bound to Galaxy (in which case the  $\langle rv_r^2 \rangle$  profile is prepared discarding the two objects),



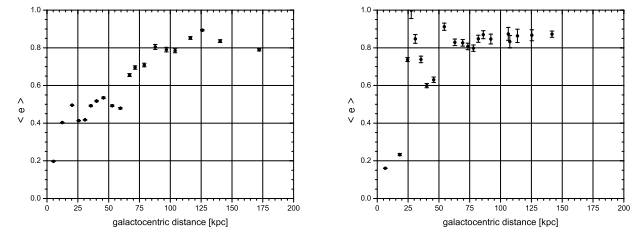
a) The radial velocity dispersions ( $r, \langle rv_r^2 \rangle / (GM)$ ) for halo compact objects prepared assuming averaging 6.8, which were the basis to obtain the phase space distribution function  $f(e, \epsilon)$



b) The  $(r, \langle rv_r^2 \rangle / (GM))$  profile [thin line], a standard deviation from the profile [dotted line], the model curve for the  $(r, \langle rv_r^2 \rangle / (GM))$  profile and its uncertainty [filled circles], and the prediction for the dispersion profile of transversal velocity  $(r, \langle rv_\phi^2 \rangle / (GM))$  [empty circles], both derived from the found distribution function  $f(e, \epsilon)$ .



c) The resulting expectation value of the symmetrized flattening parameter  $\kappa$  of the velocity dispersion ellipsoid:  $\kappa(\beta) = \frac{4}{\pi} \arctan(1 - \beta) - 1$  for a set of orbits crossing spherical shells of various radii.



d) The resulting expectation value of eccentricity for a set of orbits crossing spherical shells of various radii.

**Figure 12.** The results of applying the Keplerian ensemble method and the minimizing scheme of finding the phase space distribution function to measurements of Galactic halo compact objects: *Leo I* and *Hercules* excluded [left column]; *Leo I*, *Hercules* and *Pal 14* excluded [right column].

we obtain the following estimate of Galaxy mass:

$$M_{Gal} = 2.07 \pm 0.3 \times 10^{11} M_\odot.$$

The mass is slightly lower than necessary to gravitationally bind *Pal 14*. However, due to measurement errors of velocity and distance of *Pal 14* and the uncertainty of  $M_{Gal}$ , *Pal 14* is presumably bound to Galaxy. If *Pal 14* was assumed not bound to Galaxy, the same method would lead to  $M_{Gal} = 1.97 \times 10^{11} M_\odot$ . By assuming that only *Leo I* is not bound, we would obtain  $M_{Gal} = 2.3 \times$



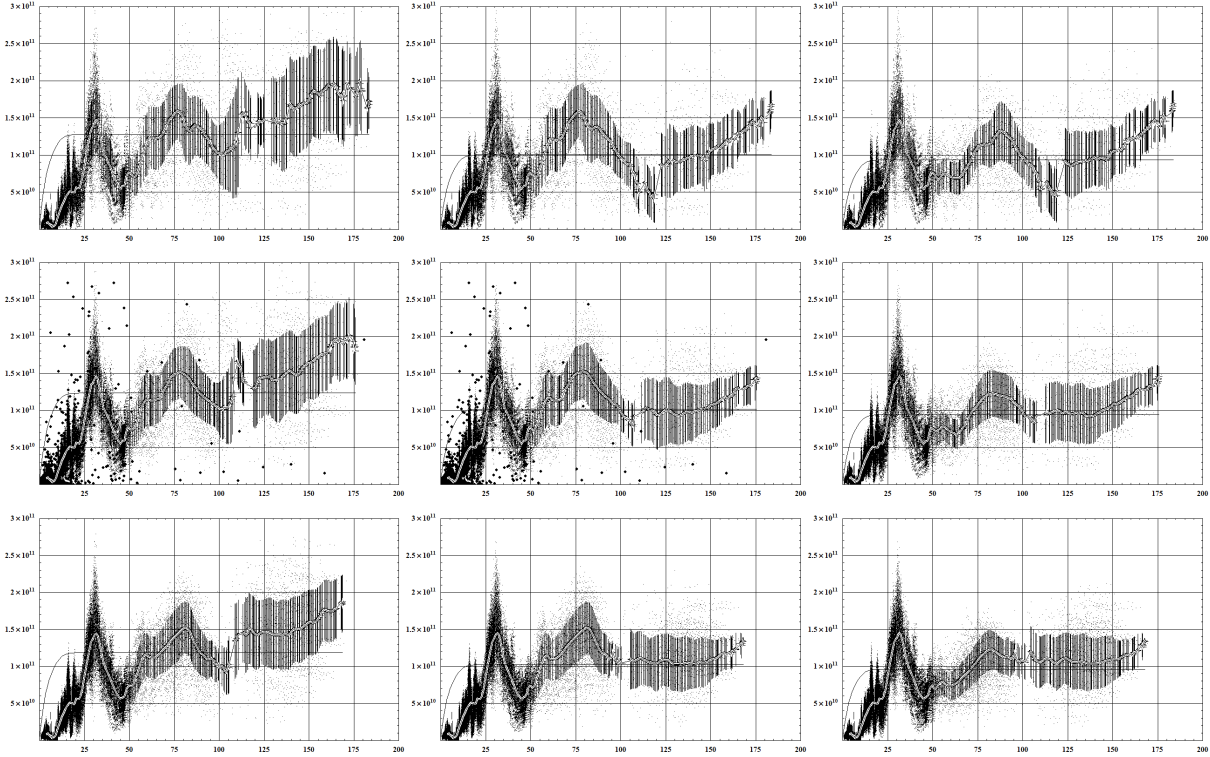


**Figure 11.** The result of the  $k$ -box averaging discussed in the text. The panels show the profiles  $(r, \langle rv_r^2 \rangle / G)$  in units  $(\text{kpc}, M_\odot)$  for halo objects obtained using  $k$ -boxes and Gaussian window of width  $w$  (symbolically,  $k, w$ ), respectively, for 5.8 [top row], 6.8 [middle row], 7.8 [bottom row], with the exclusion of *Leo I* [left column], with the exclusion of both *Leo I* and *Hercules* [middle column] and with the exclusion of *Leo I*, *Hercules* and *Pal 14* [right column].

$10^{11} M_\odot$  which is less than the escape mass for *Hercules* of about  $3 \times 10^{11} M_\odot$ .

## 5 CONCLUSIONS

We showed that the motion of halo objects regarded as test bodies in the Galactic potential well can be made consistent in the point mass approximation with Galaxy mass of about  $2.1 \times 10^{11} M_\odot$ . To achieve this result we gave up the constraint of constant anisotropy parameter. In our model the anisotropy of the velocity dispersion tensor changes with Galactocentric distance (see, Fig. 12). To some extent this is associated with variable expectation value for the ellipticity of orbits intersecting concentric spheres of various radii. In our method we did not assume the phase space distribution function, we focused on finding it based on the radial velocity dispersion of compact objects in Galaxy halo. Finding the function from this single observable might be non-unique. Our result could be tested further. To this end we presented in Fig. 12 the prediction of our model for the transverse velocity dispersion. Note, that total mass is an asymptotic notion, and dispersion functions are defined locally for all radii. Thus, whereas the mass estimate can be reliable, the behaviour of observables can be different at smaller radii, in which region one should expect a correction from higher multipoles of the real gravitational field of an extended mass distribution.

## REFERENCES

- Ackermann M., et al. 2011, Physical Review Letters, 107, 241302  
 Aprile E., et al. 2011, Phys. Rev. Lett., 107, 131302  
 Aumer M., Binney J. J., 2009, MNRAS, 397, 1286  
 Bahcall J. N., Tremaine S., 1981, ApJ, 244, 805  
 Battaner E., Garrido J. L., Membrado M., Florido E., 1992, Nature, 360, 652  
 Belokurov V., Walker M. G., Evans N. W., Faria D. C., Gilmore G., Irwin M. J., Koposov S., Mateo M., Olszewski E., Zucker D. B., 2008, ApJL, 686, L83  
 Belokurov V., Walker M. G., Evans N. W., Gilmore G., Irwin M. J., Mateo M., Mayer L., Olszewski E., Bechtold J., Pickering T., 2009, MNRAS, 397, 1748  
 Brainerd J. J., 2007, The Astrophysics Spectator, [online]  
 Bratek Ł., Sikora S., Jałocha J., Kutschera M., 2012, in preparation  
 Brown W. R., Geller M. J., Kenyon S. J., Diaferio A., 2010, AJ, 139, 59  
 Clewley L., Warren S. J., Hewett P. C., Norris J. E., Evans N. W., 2004, MNRAS, 352, 285  
 Dehnen W., Binney J., 1998, MNRAS, 294, 429  
 Dohm-Palmer R. C., Helmi A., Morrison H., Mateo M., Olszewski E. W., Harding P., Freeman K. C., Norris J., Shtetman S. A., 2001, ApJL, 555, L37  
 Eisenhauer F., et al. 2005, ApJ, 628, 246  
 Francis C., Anderson E., 2009, New Astronomy, 14, 615  
 Geha M., Willman B., Simon J. D., Strigari L. E., Kirby E. N., Law D. R., Strader J., 2009, ApJ, 692, 1464  
 Geringer-Sameth A., Koushiappas S. M., 2011, Physical Review Letters, 107, 241303  
 Harris W. E., 1996, AJ, 112, 1487  
 Honma M., Sofue Y., 1996, PASJ, 48, L103  
 Jałocha J., Bratek Ł., Kutschera M., Skindzier P., 2010, MNRAS,

- 407, 1689
- Jałocha J., Bratek Ł., Pękala J., Kutschera M., 2011, ArXiv e-prints a revised version accepted for publication in MNRAS
- Koch A., Wilkinson M. I., Kleyna J. T., Irwin M., Zucker D. B., Belokurov V., Gilmore G. F., Fellhauer M., Evans N. W., 2009, ApJ, 690, 453
- Martin N. F., Ibata R. A., Chapman S. C., Irwin M., Lewis G. F., 2007, MNRAS, 380, 281
- Mateo M. L., 1998, ARA&A, 36, 435
- Sales L. V., Navarro J. F., Abadi M. G., Steinmetz M., 2007, MNRAS, 379, 1475
- Sikora S., Bratek Ł., Jałocha J., Kutschera M., 2011, ArXiv e-prints
- Simon J. D., Geha M., 2007, ApJ, 670, 313
- Sofue Y., Honma M., Omodaka T., 2009, PASJ, 61, 227
- Starkenburg E., Helmi A., Morrison H. L., Harding P., van Woerden H., Mateo M., Olszewski E. W., Sivarani T., Norris J. E., Freeman K. C., Sheckman S. A., Dohm-Palmer R. C., Frey L., Oravetz D., 2009, ApJ, 698, 567
- Watkins L. L., Evans N. W., An J. H., 2010, MNRAS, 406, 264
- Wilhelm R., Beers T. C., Sommer-Larsen J., Pier J. R., Layden A. C., Flynn C., Rossi S., Christensen P. R., 1999, AJ, 117, 2329